Human Molecular Genetics, 2005, Vol. 14, No. 15 **2265–2276**
doi:10.1093/hmg/ddi231
Advance Access published on 29 June, 2005

Genetic dissection of Pax6 dosage requirements in the developing mouse eye

Noa Davis-Silberman[1], Tomer Kalich[1], Varda Oron-Karni[1], Till Marquardt[2], Markus Kroeber[3], Ernst R. Tamm[3] and Ruth Ashery-Padan[1,*]

[1]Sackler Faculty of Medicine, Department of Human Genetics and Molecular Medicine, Tel Aviv University, Ramat Aviv, Tel Aviv 69978, Israel, [2]The Salk Institute for Biological Studies, Gene Expression Laboratory, 10010 North Torrey Pines Road, La Jolla, CA 92037, USA and [3]Department of Human Anatomy, University of Regensburg, Universitätsstr. 31, 93053 Regensburg, Germany

Received March 9, 2005; Revised June 10, 2005; Accepted June 23, 2005

Haploinsufficiency of the transcription factor Pax6/PAX6 has been implicated in a number of congenital eye disorders in humans and mice, such as aniridia and Small-eye, which affect the development and function of the lens, cornea, anterior eye segment and neuroretina. However, the widespread distribution of Pax6/PAX6 protein within the developing and adult eye preclude the identification and direct study of the ocular tissues affected by a reduction in Pax6/PAX6 dosage. Here, we employed Cre/*loxP*-mediated inactivation of a single *Pax6* allele in either the lens/cornea or the distal optic cup to dissect the tissue-specific sensitivity to Pax6 haploinsufficiency. Exclusive inactivation of a single *Pax6* allele in the lens recapitulates the Small-eye lens and corneal defects, while only mildly affects iris morphology in a non-cell-autonomous fashion. Conversely, selective inactivation of a single *Pax6* allele in the distal optic cup revealed primarily cell-autonomous dosage requirements for proper iris differentiation, with no affects on either lens or corneal morphology. Pax6 dosage within the distal optic cup is found here to influence the number of progenitors destined for the anterior ocular structures, the timing of iris muscle-cell differentiation and iris stroma development. Taken together, we genetically dissected the complex mouse Small-eye phenotype, thereby pinpointing the underlying Pax6/PAX6 haploinsufficiency to autonomous dosage requirements within the developing iris and lens/cornea tissues.

INTRODUCTION

Most of the disorders caused by mutations in genes encoding transcription factors appear to be of dominant inheritance (1). This suggests that the cellular dosage of these factors is an important contributory determinant of their function *in vivo.* The Pax-family transcription factor, Pax6, is a highly conserved key regulator of a number of developmental processes controlling craniofacial and CNS morphogenesis, eye development and neuronal and endocrine cell-fate determination (2). Reductions in Pax6/PAX6 dosage have been shown to affect the normal development of multiple organs, making Pax6 one of the most extensively studied transcription factor in which a reduction in dosage has been shown to affect normal development (3).

Heterozygous carriers of *Pax6* mutant alleles suffer from widespread neuro-developmental anomalies including changes in the anterior commissure, reduced olfaction (4) and glucose intolerance (5). Most intensively investigated in humans is the ocular syndrome aniridia, which develops in heterozygotic carriers of *PAX6* mutations (6). Aniridia is associated with iris hypoplasia, corneal opacity, cataract formation and foveal dysplasia. More than 50% of these patients develop glaucoma. The Small-eye condition in mice and rats, likewise caused by heterozygosity for mutations in *Pax6*, represents an animal model with features that closely resemble those of human aniridia (7).

The anterior eye structures that are affected in the *Pax6* heterozygous mutants originate from three different embryonic tissues: the surface ectoderm, the neuroectoderm and the periocular mesenchyme (8,9). The lens is derived from the thickened region of the head surface ectoderm, the lens placode, which invaginates synchronously with the adjacent neuroectoderm of the optic vesicle to form the lens pit and

*To whom correspondence should be addressed. Tel: +972 36409331; Fax: +972 36409900; Email: ruthash@post.tau.ac.il

optic cup. The lens pit becomes a lens vesicle and eventually detaches from the surface ectoderm, which in turn differentiates into the corneal epithelium (8,9). The cells in the lens vesicle go on to acquire different fates according to their position. The cells located in the anterior vesicle form the monolayer of the lens epithelium, whereas those located in the posterior hemisphere of the vesicle differentiate to form the primary fibers (9). This anterior–posterior polarity of the lens cells is thought to depend on secreted factors emanating from the adjacent ocular compartments (10).

Formation of the lens placode is preceded by the expression of Pax6/PAX6 in the presumptive lens field of the head surface ectoderm (11,12). Both *Pax6* null mutants and conditional mutants selectively lacking Pax6 in the surface ectoderm, fail to develop a lens placode, thus demonstrating the central cell-autonomous role of Pax6 in establishing the lens primordium (12,13). However, Pax6/PAX6 expression is maintained in the epithelium of the adult lens, including the mitotic progenitor cells that reside predominantly in the germinative zone located at the lens equator. Pax6/PAX6 expression is reduced in the progenies of these cells upon their differentiation into lens fiber cells (14,15).

The iris and the ciliary body (CB) develop primarily from the optic cup. The inner layer of the cup differentiates mostly to the retina and the outer layer to the retinal pigment epithelium (RPE). However, the most distal tips of the cup contribute to the anterior eye structures, including the epithelial layers of the CB and iris, and to the iridal sphincter and dilator muscles (9,16). During later stages of embryogenesis and in early postnatal life, mesenchymal cells originating from the neural crest migrate and differentiate into the stroma of the CB and iris (9,17). In the mouse eye, distinct morphological changes indicating cell-fate determination to the retina or CB and iris become evident during the later stages of embryogenesis. The most distal tips of the cup start to elongate at around embryonic day 16 (E16), whereas muscle cells and the ciliary processes become apparent only close to birth (9). Formation of the anterior structures in the mouse eye is complete at about postnatal days 12–14 (P12–P14), concomitant with opening of the eyes (9). The expression of Pax6 in the developing optic cup follows a gradient from a distal high to a proximal low (18). This expression pattern suggests that a high dosage of Pax6 is required for normal development of the CB and iris. Supporting this notion is the observation that carriers of *Pax6/PAX6* mutations suffer from anterior eye malformations that include partial or complete loss of the iris.

Pax6/PAX6 is normally widely expressed during all stages of ocular development in the optic vesicle and lens placode, and during later stages in the neuroretina, as well as in the corneal and lens epithelia (11,12). Thus, it is unclear which of the multiple adjacent and interacting tissue components are directly, cell-autonomously affected by a reduction in Pax6/PAX6, and what the non-cell-autonomous effects of a reduction in Pax6 dosage. Initial studies utilizing heterozygous mice and *Pax6*(+/+) ↔ *Pax6*(+/−) chimeric mice concluded that the lens is cell-autonomously affected by the reduction in Pax6 level and that the phenotype of the $Pax6^{+/-}$ lens is the primary cause of the anterior segment abnormalities of the Pax6 heterozygous eye (19,20). This latter possibility is based on the notion that the lens plays a role in the induction of anterior ocular structures, such as the iris and CB, and on the observation that the Small-eye phenotype seems to be corrected in chimeras in which the lens epithelium is wild-type (17,20–22). In the *Pax6*(+/+) ↔ *Pax6*(+/−) chimeras, however, the *Pax6*(+/−) cells are excluded from the embryonic lens, the remaining cells are wild-type and thus the lens normal phenotype is restored (20). This restoration of the lens phenotype precluded further studies on the influence of the *Pax6*(+/−) cells on the adjacent anterior ocular structures that are affected in aniridia and Small-eye.

In the present study, we employed the Cre/*loxP* approach to selectively inactivate a single Pax6 allele in either the developing lens or the distal optic cup. We show that specific deletion of one *Pax6* copy from the lens leads to a smaller lens phenotype, thus indicating that the highly penetrant reduction in lens size occurring in Small-eye mice is due to cell-autonomous dosage requirements within the surface-ectoderm-derived tissues. However, the mono-allelic inactivation of Pax6 in the lens only mildly affects iris morphology. In contrast, specific deletion of *Pax6* in the distal optic cup revealed that Pax6 dosage in the cup is essential for normal development of the iris and is probably dispensable for the development of the adjacent lens. In the distal optic cup, Pax6 appears to play a role in defining the size of the progenitor pool destined to iris fate, in the correct timing of muscle-cell differentiation and in the formation of the iris stroma. Our results revealed almost entirely cell-autonomous Pax6 dosage requirements for both lens and iris differentiation, thus providing important insights into the etiology of the PAX6-dependent human anterior segment and lens abnormalities observed in aniridia.

RESULTS

Genetic dissection of Pax6 dosage requirements in the lens and optic cup

To investigate whether the Small-eye phenotype reflects different Pax6 dosage requirements within distinct tissue components of the eye, we employed the Cre/*loxP* approach to selectively inactivate the *Pax6* gene in either the developing lens or optic cup. For the somatic inactivation of a single *Pax6* allele upon Cre-mediated recombination, the $Pax6^{flox}$ mouse line was employed (Fig. 1A) (13). Cre-mediated recombination of the $Pax6^{flox}$ allele leads to the deletion of exons 4 through 6, the same regions deleted in the null allele for Pax6 ($Pax6^{KO}$, Fig. 1B) (23). To achieve selective inactivation of a single *Pax6* allele in the lens, we employed the *Le-Cre* transgenic mouse line. In this line, Cre is expressed under the regulation of Pax6 lens and pancreas regulatory region (Fig. 1C) (13,24). In the $Pax6^{flox/flox}$;*Le-Cre* mice, selective elimination of Pax6 expression from the lens placode and the pancreas is achieved (13,25), whereas $Pax6^{flox/+}$;*Le-Cre* embryos display a significantly reduced Pax6 levels in the lens epithelium, reflecting deletion of a single copy of *Pax6* in these cells (Fig. 2). The recombination pattern mediated by the *Le-Cre* transgenic line was characterized by crossing *Le-Cre* with the *Z/AP* reporter line, in which Cre-mediated recombination activates the expression of the human placental alkaline reporter gene (*hAP;* Fig. 1E) (26).

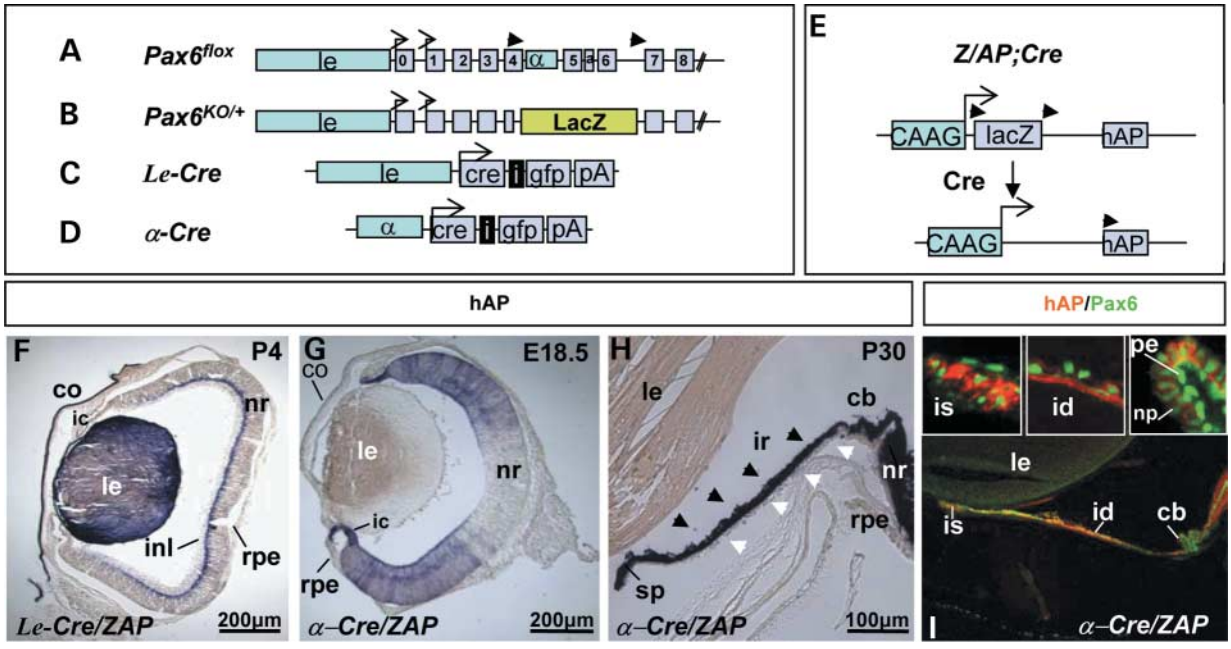

Figure 1. Transgenic lines for somatic inactivation of a single Pax6 allele. (**A**) Schematic representation of the Pax6 floxed allele (*Pax6*^{flox}). The exons are boxed. The 6.5 kb genomic region that includes the lens regulatory domain (le) and the 1.8 kb distal retina enhancer (α) are marked as blue boxes, the Pax6 transcription initiation start sites are marked by arrows, and the *loxP* sites are represented by arrowheads. (**B**) In the *Pax6*^{KO} allele, LacZ was inserted into the Pax6 locus instead of the depicted exons (**C**). The *Le-Cre* transgene contains the lens regulatory region and (**D**) *α-Cre* transgene includes the α enhancer; both are followed by the *Cre* gene, the internal ribosome-binding site (i), *gfp* and poly A. (**E**) The *Z/AP* transgene construct before and after Cre-mediated recombination. In double-positive progeny, Cre-mediated recombination eliminates the *LacZ* sequence, enabling the expression of the reporter gene *human alkaline phosphatase* (*hAP*). (**F**) The recombination pattern mediated by *Le-Cre* is evident in all lens cells, as well as in the corneal and eyelid epithelia (data not shown). Recombination is also detected in a subpopulation of amacrine cells at the inner nuclear layer. *Le-Cre*-mediated recombination does not occur in the iris or ciliary body (CB). (**G**) hAP staining of E18.5 *α-Cre;Z/AP* eyes demonstrates Cre activity throughout the distal neuroretina, including the most distal tips, destined for the iris and the CB. (**H**) In adult mice, the epithelial layer (black arrowheads) of the iris and CB epithelium express hAP. No staining is detectable in the stromal cells of the iris (white arrowheads) or the CB. (**I**) Double-immunolabeling with antibodies specific for Pax6 (green) and hAP (red) demonstrate hAP activity in the Pax6^{+} epithelial layer of the CB (but not in the pigmented Pax6^{+} layer, right upper inset), and in the sphincter and dilator muscle (left and middle upper insets, respectively). a, alternatively spliced exon 5a; cb, ciliary body; co, cornea; ic, iris and ciliary body progenitors; id, iris dilator; inl, inner nuclear layer; ir, iris; is, iris sphincter; le, lens; np, non-pigmented epithelium; nr, neuroretina; pe, pigmented epithelium; rpe, retinal pigment epithelium.

Characterization of hAP activity in *Le-Cre;Z/AP* mice revealed the presence of recombinant cells in the lens and cornea and in cells of the inner nuclear layer within the proximal neuroretina (Fig. 1F) (13,27). However, no recombination could be detected at any stage analyzed within the iris (Fig. 1F).

For specific deletion of a single *Pax6* allele in the optic cup, we employed the *α-Cre* mouse line that expresses Cre under the regulation of the Pax6 distal retina enhancer (Fig. 1D) (24,28). In the *Pax6*$^{flox/+}$*;α-Cre* embryos, reduced levels of Pax6 within the iris primordium were detected (Fig. 3). Characterization of hAP in the *α-Cre;Z/AP* embryos revealed recombinant cells throughout the distal optic cup, including the most distal tips that develop to the adult CB and iris structures (Fig. 1G) (28). In the adult *α-Cre;Z/AP* mice, hAP was indeed detected in the inner epithelial layers of the iris and the CB, as well as in the sphincter and dilator muscle cells (Fig. 1H and I). However, in the *α-Cre;Z/AP* mice, the hAP was not detected in the lens, the stromal cells of the iris, the CB, the pigmented cells of the CB or in the RPE (Fig. 1H and I). Thus, comparison of the phenotypes of the *Pax6*$^{KO/+}$ mice (23) to the two somatic mutants (*Pax6*$^{flox/+}$*;Le-Cre* and *Pax6*$^{flox/+}$*;α-Cre*) allowed us to dissect the Pax6 dosage requirements within the developing lens and iris compartments.

Selective reduction of Pax6 dosage in the lens recapitulates the *Pax6*$^{+/-}$ small lens and cornea phenotypes

Previous analysis of the ocular phenotype of *Pax6* heterozygous mutants revealed an early delay in the formation of the lens placode, resulting in the eventual formation of smaller lenses (19). Attachments between the lens and the cornea were also attributed to the reduction in Pax6 dosage (19,29). Moreover, it was suggested that changes in the lens may be the indirect, non-cell-autonomous cause of iris hypoplasia (20,22). To investigate cell-autonomous and non-cell-autonomous Pax6 dosage requirements, we first studied lens development in *Pax6*$^{flox/+}$*;Le-Cre* and *Pax6*$^{flox/+}$*;α-Cre* versus *Pax6* mutant mice (*Pax6*$^{KO/+}$) (23) and control littermates, respectively. The inactivation of a single allele could result in an up-regulation of expression of the wild-type *Pax6* allele or could be compensated for by cells that escape Cre-mediated deletion (20). Therefore, we evaluated Pax6 levels by confocal imaging of Pax6 immunofluorescence in *Pax6*$^{flox/+}$*;Le-Cre* and *Pax6*$^{flox/+}$*;α-Cre* eyes at E14.5 (Figs 2 and 3). Using polyclonal antibodies directed against Pax6, we measured the relative fluorescence intensity from the center of the lens epithelium (red square; Fig. 2C) of *Pax6*$^{flox/+}$*;Le-Cre* embryos and *Pax6*$^{flox/+}$ control littermates (Fig. 2A–D). To eliminate

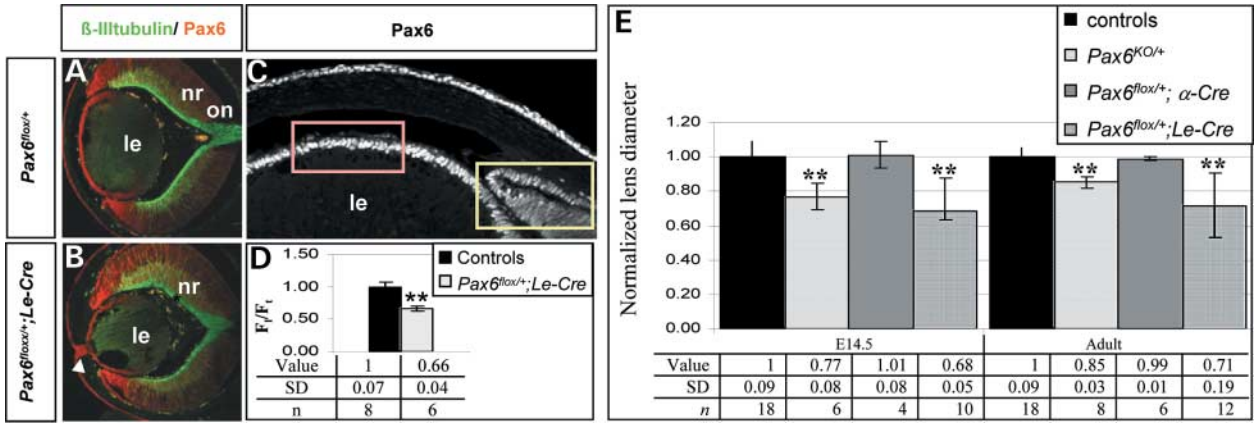

Figure 2. Reduction in Pax6 dosage in the lens results in a smaller lens and adhesions between the lens and cornea. (**A**–**C**) Pax6 (red) staining intensity evaluated at E14.5 by confocal microcopy of serial sections from eyes of control (A and C) and *Pax6*$^{flox/+}$*;Le-Cre* (B) embryos. Pax6 average pixel intensity was measured from the center of the lens epithelium (measurements from region marked as red box, C) and normalized by division by the intensity detected in the retinal distal tips (measurements from region marked as yellow box, C). (**D**) The normalized intensity (fluorescent intensity in the lens epithelium/fluorescent intensity in the distal tips; F_l/F_t) of Pax6 in the *Pax6*$^{flox/+}$*;Le-Cre* eyes was reduced to 66% of normal. The table summarizes the data for each genotype including the normalized values, number of eyes and the standard deviation (SD). (A and B) Adhesions between the lens and the cornea are not detectable in the E14.5 control embryos (A) but can be seen in some sections of the *Pax6*$^{flox/+}$*;Le-Cre* eyes (B, arrowhead). (**E**) A significant reduction to 68 and 71% of normal was observed in the lens diameter of *Pax6*$^{flox/+}$*;Le-Cre* mice at E14.5 and adulthood, respectively. At the same stages, lens diameter was reduced to 77 and 85% of normal in *Pax6*$^{KO/+}$ mice and did not vary significantly in *Pax6*$^{flox/+}$*α-Cre* mice. $^{**}P < 0.001$. Controls were *Pax6*$^{flox/+}$ (littermates of *Pax6*$^{flox/+}$*;Le-Cre* mice), *Pax6*$^{+/+}$ (littermates of *Pax6*$^{KO/+}$ mice) or *Pax6*$^{+/+}$*;α-Cre* (littermates of *Pax6*$^{flox/+}$*;α-Cre* mice). le, lens; nr, neuroretina; on, optic nerve.

possible variability between slices, the average fluorescence intensities in each section were divided by the average fluorescence intensities in the adjacent optic cup tips (yellow square; Fig. 2C), in which the Pax6 gene was not mutated. This analysis showed a 34% reduction in Pax6 levels in *Pax6*$^{flox/+}$*;Le-Cre* compared with *Pax6*$^{flox/+}$ controls (Fig. 2D), thus demonstrating the efficient inactivation of one Pax6 copy in the lens epithelium. The selective lens/cornea-specific reduction in Pax6 dosage resulted in the lens remaining attached to the cornea (Fig. 2B). This attachment recapitulates the defect observed in human Peter's anomaly patients and in Pax6 Small-eye mice (30,31), thus demonstrating the cell-autonomous Pax6 dosage sensitivity of the surface ectoderm for the morphogenetic separation of lens and cornea.

The lens has been shown to play a central role in the development of the anterior segment, whereas lens growth depends on growth factors secreted from the CB, iris and retina into the aqueous and vitreous compartments (10). Pax6 is expressed in both the developing lens and the optic cup, and several studies have indicated cell-autonomous requirements for normal Pax6 dosages in lens development (20,29,32). However, these findings did not exclude the possible contribution of Pax6 dosage sensitivity in the optic cup to lens growth or differentiation.

To address this issue, we compared lens size at mid-embryogenesis (E14.5) of embryos heterozygous for the *Pax6* null allele (*Pax6*$^{KO/+}$), heterozygous for Pax6 deletion in the lens (*Pax6*$^{flox/+}$*;Le-Cre*) and heterozygous for Pax6 deletion in the distal optic cup (*Pax6*$^{flox/+}$*;α-Cre*). A reduction in lens size to 77 and 68% of normal was observed in the *Pax6*$^{KO/+}$ and the *Pax6*$^{flox/+}$*;Le-Cre*, respectively, whereas no significant change in lens size was observed in the *Pax6*$^{flox/+}$*;α-Cre* E14.5 embryos (Fig. 2E; E14.5). These results indicate that the reduced lens size observed in the *Pax6*$^{KO/+}$ at E14.5 is due exclusively to cell-autonomous Pax6 dosage requirements within the lens. We next asked whether the growth of the lens during later stages of embryogenesis and postnatal stages is influenced by Pax6 dosage reduction in the adjacent iris and CB. For this, the lens diameter was measured in adult (P30) *Pax6* $^{KO/+}$, *Pax6*$^{flox/+}$*;Le-Cre, Pax6*$^{flox/+}$*;α-Cre* and control mice (Fig. 2E; Adult). A reduction in lens diameter to 85 and 71% of normal was observed in the *Pax6*$^{KO/+}$ and the *Pax6*$^{flox/+}$*;Le-Cre* mice, respectively, whereas the diameter of the *Pax6*$^{flox/+}$*;α-Cre* lenses remained similar to that of the controls (Fig. 2E; Adult). We thus concluded that lens development is solely dependent on Pax6 dosage in the lens and is insensitive either to its dosage in the optic cup or to the iris abnormalities caused by this reduction in the adjacent anterior segment of the eye.

Pax6 distribution along the optic cup in a distal^{high}–proximal^{low} gradient, and its correlation with non-neuronal and neuronal cell fates

Pax6 graded expression in the optic cup raises the possibility that the differential levels of expression are correlating with the various phenotypes acquired by the optic cup progenitors. In particular, we wanted to characterize Pax6 dosage changes in the distal optic cup that is mutated in the *Pax6*$^{flox/+}$*;α-Cre*, and correlate them with the fates of the neuronal and non-neuronal progenitor of the neuroretina and the anterior ocular segment, respectively. β-III tubulin is expressed in post-mitotic neurons (33) while being excluded from the iris and CB primordium. To characterize the relation between Pax6 expression levels and the neuronal and the non-neuronal compartments of the optic cup, specific primary antibodies against Pax6 and β-III tubulin were employed to detect the two proteins on embryo sections (see Materials and Methods and Fig. 3). The averaged normalized intensity of Pax6 staining in four different regions (d1–d4, Fig. 3) along the distal–proximal axis was calculated. In the controls, quantitative analysis using confocal microscopy revealed a high Pax6

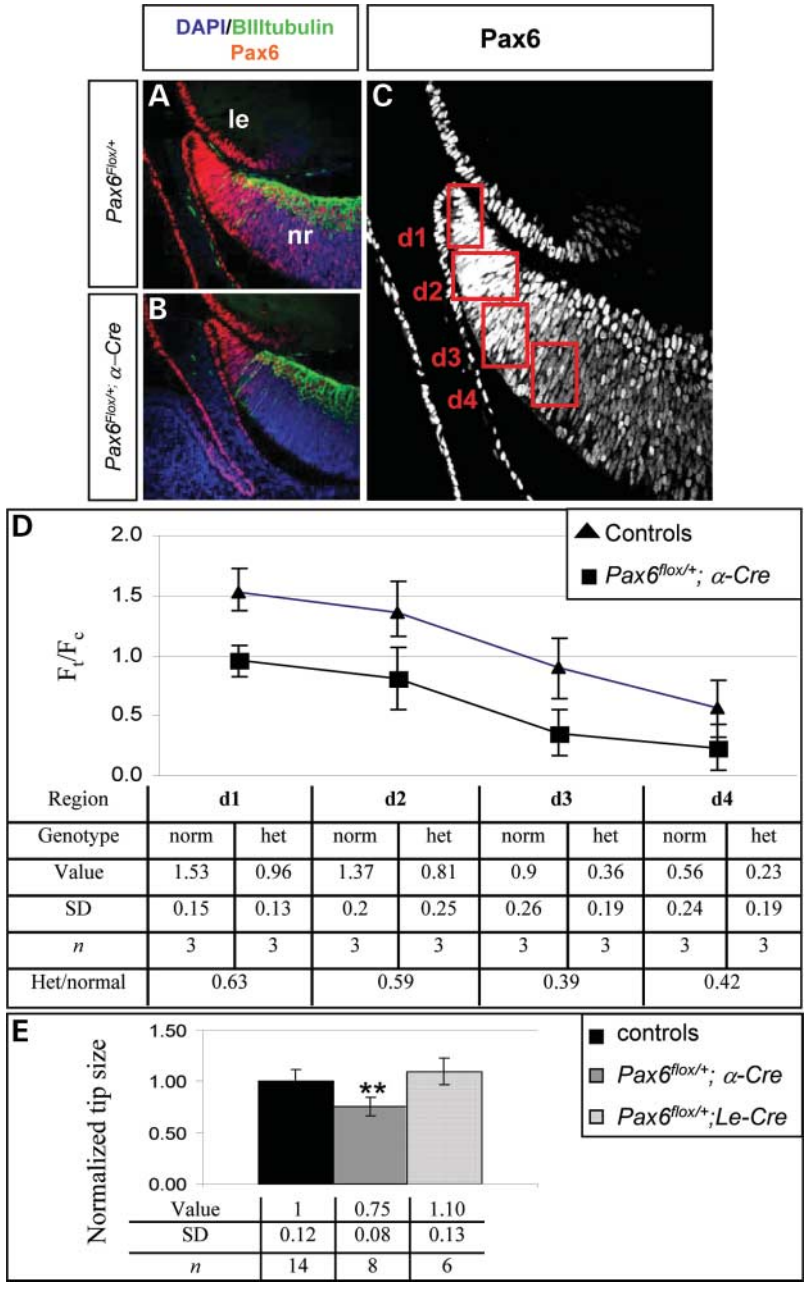

Region	d1		d2		d3		d4	
Genotype	norm	het	norm	het	norm	het	norm	het
Value	1.53	0.96	1.37	0.81	0.9	0.36	0.56	0.23
SD	0.15	0.13	0.2	0.25	0.26	0.19	0.24	0.19
n	3	3	3	3	3	3	3	3
Het/normal	0.63		0.59		0.39		0.42	

Value	1	0.75	1.10
SD	0.12	0.08	0.13
n	14	8	6

Figure 3. Reduction in Pax6 dosage in the distal retina results in a smaller pool of iris progenitor cells at E14.5. (**A** and **B**) Pax6 (red) is strongly expressed in the distal part of the E14.5 retina. Its expression decreases gradually toward the proximal retina, where neuronal cell differentiation has been initiated, as indicated by the expression of β-III tubulin (green). The Pax6–distal^{high}–proximal^{low} gradient is detected in both (A and **C**) control and (B) *Pax6$^{flox/+}$;α-Cre* mutant E14.5 eyes (**D**). (B) In the *Pax6$^{flox/+}$;α-Cre* eyes, however, the absolute levels of expression along the distal–proximal axis are reduced. The average normalized intensity of Pax6 staining at four different regions (d1–d4) along the distal–proximal axis was calculated. The most distal tips were defined by d1, whose region was arbitrarily defined as 72 pixels from the tips. The area of d2 covers the rest of the tips up to the border with the β-III tubulin-expressing cells. The d3 and d4 regions were each arbitrarily defined as 72 pixels in length and were located in the region of retinal progenitor cells. Values were normalized by dividing them by the averaged pixel intensity of Pax6 in the cornea, which remained unchanged in the mutants. (D) Normalized intensities for each area (d1–d4) of controls (triangles) and *Pax6$^{flox/+}$;α-Cre* (squares) are presented (fluorescent intensity in the distal tips/fluorescent intensity in the cornea; F_t/F_c). The table summarizes the data for each area including the normalized values, number of eyes and the standard deviation. (**E**) A significant reduction to 75% of normal was observed in the retinal tips area of *Pax6$^{flox/+}$;α-Cre* embryos at E14.5. No reduction was seen in the retinal tips area of *Pax6$^{flox/+}$;Le-Cre* embryos. $^{**}P < 0.001$. Controls were *Pax6$^{flox/+}$* (littermates of *Pax6$^{flox/+}$;α-Cre* or *Pax6$^{flox/+}$;Le-Cre* mice). le, lens; nr, neuroretina.

dosage in the most distal tips (Fig. 3). With increasing distance from the tips, Pax6 dosage gradually declined from an average fluorescence intensity of 1.53 at the most distal tips (defined as d1, Fig. 3C and D) to an average pixel intensity of 0.9 at the border with the distal-most extent of β-III tubulin expression (defined as d3, Fig. 3C and D) and down to an average pixel intensity of 0.56 in progenitor cells located further toward the center of the neuroretina (defined as d4, Fig. 3C,D).

To verify the dosage reduction of Pax6 at this stage, we compared Pax6 protein distribution in the E14.5 *Pax6$^{flox/+}$;α-Cre* optic cup to that in their control *Pax6$^{flox/+}$* littermates. In the optic cups of *Pax6$^{flox/+}$;α-Cre* mice, the slope of the gradient was maintained and was similar to that of the controls. However, the average intensity at each point was significantly lower and ranged from an averaged intensity of 0.96 pixel at d1 to an average of 0.36 pixel intensity at d3 and down to 0.23 pixel intensity at d4 (Fig. 3D). The average reduction in Pax6 levels across the distal optic cup of *Pax6$^{flox/+}$;α-Cre* when compared with *Pax6$^{flox/+}$* was down to 63% in d1, 59% in d2, 39% in d3 and 42% in d4, confirming that only one *Pax6* allele was active in the *Pax6$^{flox/+}$;α-Cre* mutant retina (Fig. 3D).

Pax6^{high} in the E14.5 optic cup as a critical size determinant of the progenitor pool that differentiates to anterior eye structures

The elevated expression of Pax6 in the distal optic cup suggests that the iris progenitors are sensitive to its dosage. To investigate this further, we measured the size of the distal tips of the optic cup, including the iris primordium, as defined by the absence of the neuronal marker β-III tubulin (Fig. 3E) in the E14.5 *Pax6$^{flox/+}$;α-Cre* when compared with control *Pax6$^{flox/+}$* littermates. Interestingly, the retinol cup tips of the *Pax6$^{flox/+}$;α-Cre* embryos were found to be significantly reduced in size compared with control littermates at E14.5 (75% of *Pax6$^{flox/+}$*, Fig. 3B and E). In addition, a proportionate decrease in the number of cells within the distal optic cup of *Pax6$^{flox/+}$;α*-Cre when compared with control *Pax6$^{flox/+}$* was observed (78% of control, SD = 0.09, n=6 eyes for *Pax6$^{flox/+}$;α-Cre;* SD = 0.06, n=4 for *Pax6$^{flox/+}$*; $P < 0.001$), thus indicating a reduction in the pool of cells destined to anterior eye structures. To asses whether this observed reduction is specific to the distal optic cup or results from a general decrease in the number of both the neuronal and the non-neuronal optic cup mutant progenitors, the number of Cre-expressing cells was determined in the *Pax6$^{flox/+}$;α-Cre* and *Pax6$^{+/+}$;α-Cre* embryos. Co-expression of green fluorescent protein (GFP) with the Cre protein enabled us to evaluate the total number of cells expressing Cre in *Pax6$^{flox/+}$;α-Cre* and *Pax6$^{+/+}$;α-Cre* embryos by counting, using fluorescence-activated cell sorting (FACS), the average number of GFP-positive (GFP$^+$) cells per embryo for these genotypes. A mild but not significant reduction in the average number of GFP$^+$ cells per embryo was found between the two genotypes in E14.0 embryos (in the *Pax6$^{+/+}$;α-Cre* 38 885 GFP$^+$ cells/embryo, SD = 13 977, n = 488 embryos and in the *Pax6$^{flox/+}$;α-Cre* 35 544 GFP$^+$ cells/embryo, SD = 11 379, n = 465 embryos). The mild reduction in the number of GFP$^+$ cells in the *Pax6$^{flox/+}$;α-Cre* mutants is consistent with the observed reduction in the size of the relatively small pool of non-neuronal progenitor cells destined to an iris fate rather than with a general decrease in the size of both the neuronal and non-neuronal progenitors.

The lens has been previously suggested to induce and influence the growth of anterior ocular structures (21,22,34). Therefore, we tested whether the reduction in Pax6 dosage in the *Pax6$^{flox/+}$;Le-Cre* lenses would lead to defects in patterning of the adjacent distal optic cup during mid-gestation (E14.5). Evaluation of the size of the anterior ocular progenitor pool, as described earlier for the E14.5 *Pax6$^{flox/+}$;α-Cre* eyes, revealed no significant reduction (Fig. 3E). This observation indicated that Pax6 levels in the lens do not influence indirectly the formation of iris primordium.

Reduction in Pax6 dosage in the distal optic cup results in iris hypoplasia

The reduction in iris primordium in the E14.5 *Pax6$^{flox/+}$;α-Cre* optic cup suggested that the iris phenotype in Small-eye mice and aniridia patients results from cell-autonomous Pax6 dosage requirements in the distal optic cup. To examine this possibility, we first measured changes in iris size during late embryogenesis (E17.5) and early postnatal stages (P4) in the *Pax6$^{flox/+}$;α-Cre* and control littermates. During late embryogenesis (E17.5), the distal tips, including the prospective iris and CB, were significantly reduced in length and width in the *Pax6$^{flox/+}$;α-Cre* embryos (to 83 and 72% of controls, respectively) (Fig. 4D and G and data not shown). The reduction in the iris length became more pronounced during early postnatal stages (to 62% of control at P4) (Fig. 4E), a time when the iris elongates and the ciliary processes start to form, while the CB size appeared normal at this stage (data not shown). We investigated the possibility of iris hypoplasia by measuring the iris length in the adult *Pax6$^{flox/+}$;α-Cre* and littermates *Pax6$^{flox/+}$* control eyes. The average length of the adult mutant iris was indeed significantly reduced to 79% of that of the control (Fig. 4F and G), whereas the rest of the eyecup appeared to be of normal size. This finding showed, for the first time, that a considerable part of the iris phenotype in Small-eye mice and in aniridia patients results from cell-autonomous functioning of Pax6 in the embryonic distal optic cup.

Pax6 dosage in the distal optic cup is required for the onset of iris smooth muscle-cell differentiation

The iris in the adult is composed of three cellular layers: the inner pigmented epithelium, a layer of smooth muscle cells and the outer stroma. We examined the expression of Pax6 in these adult structures. Pax6 expression was maintained in the two inner layers, i.e. in the iris pigment epithelium and in the muscle-cell layer (Fig. 5A). These layers of the iris were expected on the basis of hAP activity monitored in the *Pax6$^{flox/+}$;α-Cre;Z/AP* (Fig. 1) to be heterozygous for the mutated Pax6 allele in the *Pax6$^{flox/+}$;α-Cre* mice. Therefore, we tested whether the reduced Pax6 dosage affects the differentiation of muscle cells. Using specific antibodies, we monitored the distribution of smooth-muscle actin (Sma)-expressing cells during the early stages of muscle-cell formation (P4, Fig. 5D and E) and in adult *Pax6$^{flox/+}$;α-Cre* and control *Pax6$^{flox/+}$* mice (Figs 5F and 6 K, I). The proportion of Sma-positive cells was significantly lower (45% of controls) in P4 *Pax6$^{flox/+}$;α-Cre* mice (Fig. 5F). However, in adult *Pax6$^{flox/+}$;α-Cre* eyes, the proportion of Sma-positive cells relative to iris number of cells was similar to that of control littermates (Fig. 5F). This observation suggests that

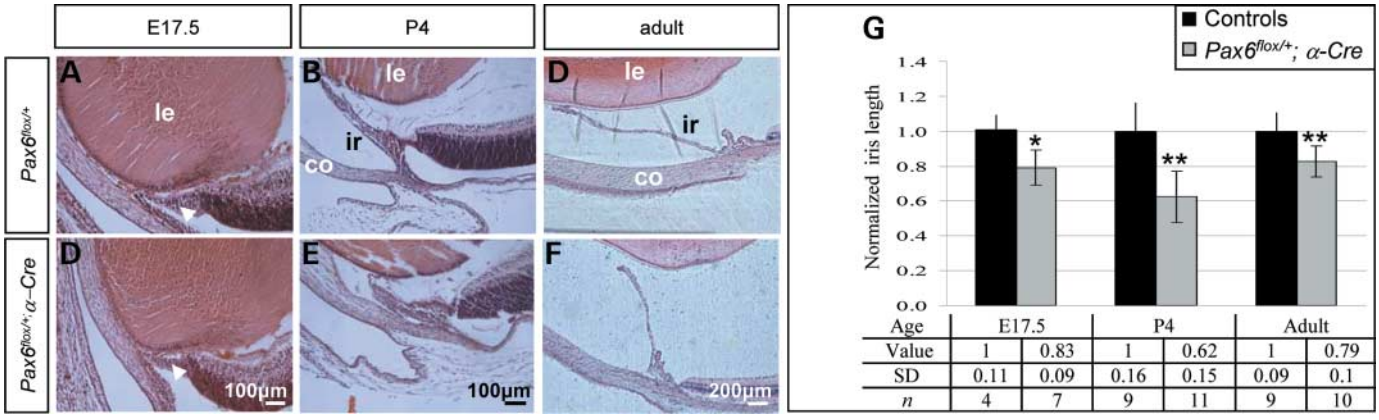

Age	E17.5		P4		Adult	
Value	1	0.83	1	0.62	1	0.79
SD	0.11	0.09	0.16	0.15	0.09	0.1
n	4	7	9	11	9	10

Figure 4. Pax6 dosage in the distal optic cup influences iris size. Hematoxylin and eosin (H&E) staining of (**A**–**E**) paraffin or (C and **F**) plastic sections of eyes of E17.5 (A and D), P4 (B and E) and adult (2 weeks-6 months; C and F) mice demonstrate reduction in the developing and mature iris length in eyes of *Pax6*$^{flox/+}$;*α-Cre* mice (D–F) relative to control mice (A–C). (A and D) At E17.5, the prospective iris and CB (white arrow) are defined as the tips of the optic cup, which does not show neuronal histology or expression of the neuronal marker β-III tubulin (tested on an adjacent section, data not shown). (**G**) Quantitative analysis of iris length showed significant reductions (to 83, 62 and 79% of normal) at E17.5, P4 and adulthood, respectively. Values normalized to controls, numbers of eyes and standard deviations are presented in the table. $^{*,**}P < 0.01$ and $P < 0.001$, respectively. Controls were *Pax6*$^{flox/+}$ (littermates of *Pax6*$^{flox/+}$;*α-Cre* mice). co, cornea; ir, iris; le, lens.

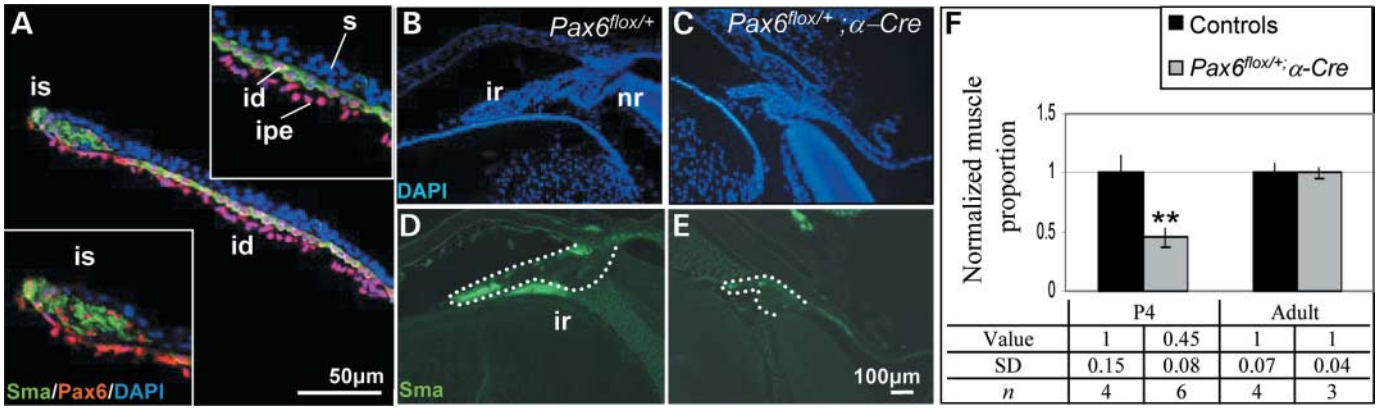

	P4		Adult	
Value	1	0.45	1	1
SD	0.15	0.08	0.07	0.04
n	4	6	4	3

Figure 5. Delay in smooth muscle-cell differentiation in *Pax6*$^{flox/+}$;*α-Cre* postnatal mutants is compensated for during later stages of development. (**A**) Pax6 (red) is detected in two cellular layers of the adult iris; the inner iris pigmented epithelium and the middle layer that co-expresses smooth-muscle actin (Sma; green) counterstained with DAPI (blue) shows iris morphology. Enlargements of the iris sphincter and dilator are shown in the insets. (**B**–**E**) Sma staining at P4 demonstrates a decrease in the proportion of the iris muscle layer in *Pax6*$^{flox/+}$;*α-Cre* mutants (C and E) when compared with littermate controls (B and D). (**F**) Quantitative analysis of iris muscle proportion showed a significant reduction to 45% of normal in *Pax6*$^{flox/+}$;*α-Cre* at P4. In adulthood, the iris muscle layer reaches normal proportions. Values normalized to controls, numbers of eyes and standard deviations are presented in the table. $^{**}P < 0.001$. Controls were *Pax6*$^{flox/+}$ (littermates of *Pax6*$^{flox/+}$;*α-Cre* mice). co, cornea; id, iris dilator; ipe, iris pigment epithelium; ir, iris; is, iris sphincter; nr, neuroretina; s, iris stroma.

the onset of muscle-cell differentiation is initially delayed and that during later stages, there is growth compensation leading to a relatively normal formation of the iris muscle cell types.

Pax6 dosage is required autonomously in the lens and iris for their normal development

The previous results revealed the effect of Pax6 reduction on the embryonic lens and optic cup. We thus evaluated pupil and iris function and morphology and the whole eye appearance in adult *Pax6*$^{KO/+}$, *Pax6*$^{flox/+}$;*α-Cre* and *Pax6*$^{flox/+}$;*Le-Cre* mice when compared with their control littermates. For this, eyes were enucleated and the pupil was observed after administration of pilocarpine to obtain maximal iris constriction (Fig. 6A–D). In *Pax6*$^{flox/+}$ controls, the pupil was rounded and centered (white arrow in Fig. 6A), whereas in the *Pax6*$^{KO/+}$ mice, the pupil was irregular and enlarged, indicating of an iris hypoplasia (white arrow, Fig. 6B and reference 7). Furthermore, in the *Pax6*$^{KO/+}$ eyes, adhesions between the lens and the cornea were detected, resulting in opaque regions in the normally transparent lens and cornea (black arrow Fig. 6B and reference 7). Analysis of the *Pax6*$^{flox/+}$;*α-Cre* pilocarpine-treated eyes did not reveal abnormalities in the lens or cornea (Fig. 6C). However, in agreement with the observed developmental defect in iris growth in the *Pax6*$^{flox/+}$;*α-Cre* (Fig. 4), a substantial increase in pupil diameter was observed when compared with controls (white arrow, Fig. 6C). However, in contrast with the obvious

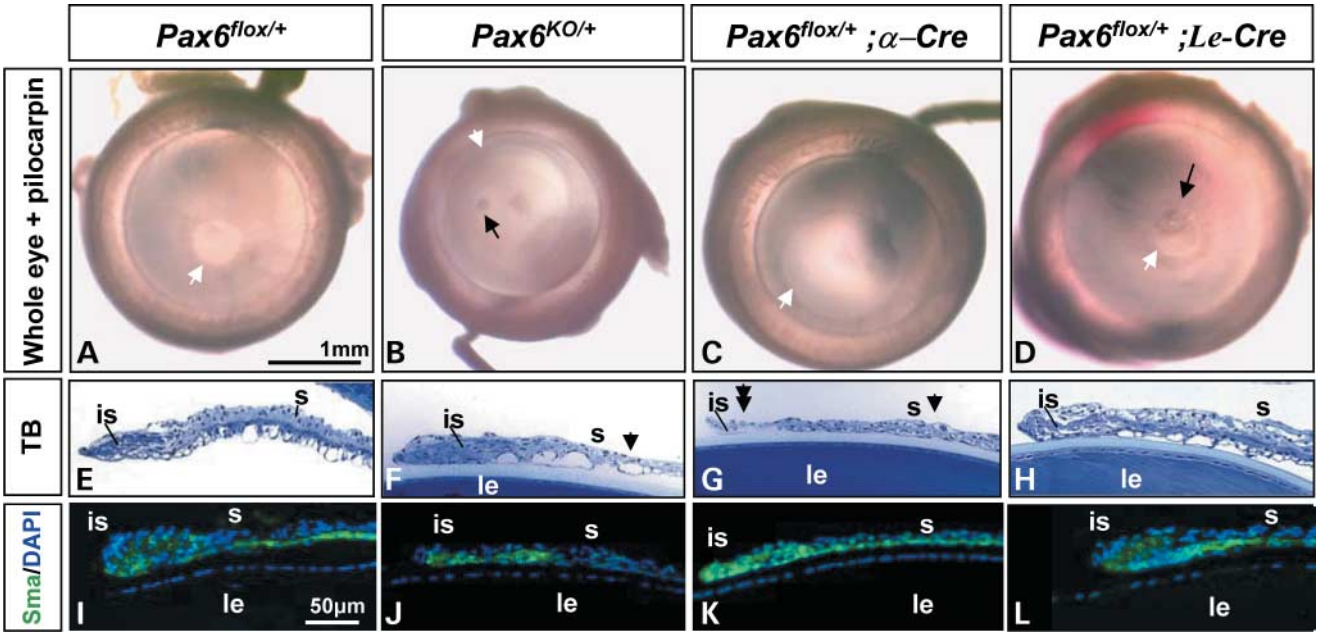

Figure 6. Iris hypoplasia is primarily due to the functions of Pax6 in the optic cup. Examination of pilocarpine-treated (**A**–**L**) adult mouse eyes (P30) of *Pax6*$^{flox/+}$ (A, E, I), *Pax6*^{KO} (B, F, J), *Pax6*$^{flox/+}$*;α-Cre* (C, G, K) and *Pax6*$^{flox/+}$*;Le-Cre* (D, H, L) for pupil morphology (A–D), iris sphincter histology (E–H) and expression of Sma (I–L). Enlarged pupils are observed in the *Pax6*$^{flox/+}$*;α-Cre* and *Pax6*^{KO} (B, C) but not in the *Pax6*$^{flox/+}$*;Le-Cre* (D) when compared with the control *Pax6*$^{flox/+}$ (A) mice. The white arrows (A–D) point to the pupil, the black arrows to the attachments between the cornea and lens (B and D). No apparent differences with respect to iris histology can be observed between *Pax6*$^{flox/+}$ control and *Pax6*$^{flox/+}$*;Le-Cre* mice (A and D). In contrast, the iris stroma is markedly thinner in *Pax6*$^{KO/+}$ and *α-Cre* mice (black arrowheads in F and G). In *Pax6*$^{flox/+}$*;α-Cre* mice, the sphincter of the iris is noticeably thinner than control (double arrowheads in G). Sma is detected in all genotypes (counterstained with DAPI in blue, I–L). is, iris sphincter; le, lens; s, iris stroma; TB, toluidine blue.

iris phenotype of the *Pax6*$^{KO/+}$ and *Pax6*$^{flox/+}$*;α-Cre* mice, in the *Pax6*$^{flox/+}$*;Le-Cre* pilocarpine-treated eyes, the pupil was small and iris hypoplasia was not observed. In the *Pax6*$^{flox/+}$*;Le-Cre* embryos, the adhesions between the lens and cornea were evident (black arrow, Fig. 6D), as expected from the attachment between these two structures observed in mid-embryogenesis (Fig. 2).

For a detailed study of the iris phenotypes, we conducted a histological analysis of semi-thin sections of the iris and monitored the expression of Sma in *Pax6*$^{flox/+}$, *Pax6*$^{KO/+}$, *Pax6*$^{flox/+}$*;α-Cre* and *Pax6*$^{flox/+}$*;Le-Cre* eyes. The morphology of the iris sphincter of *Pax6*$^{flox/+}$*;α-Cre* was similar to that of the *Pax6*$^{KO/+}$, as both being thinner than normal (Fig. 6G and F), although the expression of Sma was maintained in both *Pax6*$^{KO/+}$ and *Pax6* $^{flox/+}$*;α-Cre* irises (Fig. 6J and K). Interestingly, the histological analysis (Fig. 6E–H) (7) revealed a marked decrease in the thickness of the iris stroma in the *Pax6*$^{KO/+}$ and *Pax6* $^{flox/+}$*;α-Cre* irises (arrowheads in Fig. 6F and G) when compared with the *Pax6*$^{flox/+}$control (Fig. 6E). Finally, although deviations from the round shape and irregular rim were observed in some of the examined *Pax6*$^{flox/+}$*;Le-Cre* eyes (data not shown), the structure of the sphincter showed no obvious differences between *Pax6*$^{flox/+}$*;Le-Cre* mice and their *Pax6*$^{flox/+}$ control littermates: the iris was of comparable thickness in both groups, and no obvious signs of iris atrophy or hypoplasia or abnormal expression of Sma were detected (Fig. 6H and L). Taken together, these findings demonstrate that most aspects of the mouse Small-eye and human aniridia iris phenotypes likely result from Pax6 dosage requirements within the distal optic cup. Pax6 dosage in the iris primordium probably affects iris phenotype in two ways: first, it determines the size of the progenitor cells destined to an iris fate and secondly, it influences the development of the iris stroma.

DISCUSSION

Aniridia belongs to a genetically heterogeneous group of developmental disorders, a main feature of which is ocular anterior segment dysgenesis resulting in impaired vision and a high susceptibility to developing glaucoma (35). The aniridia phenotype has variable expressivity and incomplete penetrance, which reflects the complex developmental process that leads to the genesis of the eye anterior segment (36). To elucidate the underlying complexity of this multi-factorial human phenotype, we utilized the Cre/*loxP*-mediated tissue-specific gene inactivation in mice to dissect the ocular components susceptible to Pax6 haploinsufficiency. The findings provide some important insights into the etiology of aniridia. Selective monoallelic deletion of *Pax6* from the lens and cornea mimicked the Small-eye phenotype of the murine counterpart of human aniridia including reduced lens size and adhesion of lens and cornea. In contrast, the exclusive deletion of one *Pax6* allele within the distal optic cup mimicked most aspects of Small-eye and aniridia iris phenotypes without affecting the lens or cornea. Interestingly, the high dosage of Pax6 in the peripheral optic cup is demonstrated here to be required for the size of the iris primordium and for the normal timing of iris muscle-cell differentiation.

Thus, the coordinate development of the lens and iris, which is crucial for normal ocular function, is mediated primarily by autonomous requirements for Pax6 dosages in each of the two adjacent tissue types.

Cell-autonomous Pax6 haploinsufficieny in lens development

The regulation of *Pax6* expression is mediated by multiple transcriptional regulatory control regions (24,37–42). A direct *in vivo* functional study was conducted on the upstream *Pax6* ectoderm enhancer (*EE*) (29), which mediates *Pax6* expression in the surface ectoderm during lens placode formation and early stages of lens and cornea development (E9–E12). Deletion of the *EE* sequence resulted in a mild lens phenotype, consistent with important activity of additional lens enhancers. The Cre expression mediated by the *Le-Cre*-transgenic line is driven by a genomic region that includes the *EE* enhancer. In contrast with the mild $Pax6^{\Delta EE/\Delta EE}$ phenotype, the $Pax6^{flox/flox}$*;Le-Cre* mutation results in irreversible inactivation of *Pax6* from cells in which the Cre was active and from their progeny, i.e. the lens placode stage. The recapitulation of the Small-eye lens/cornea phenotype in the $Pax6^{flox/+}$*;Le-Cre* mice suggests that Pax6 dosage is crucial for normal lens development from the lens placode stage onwards. This dosage sensitivity may be more pronounced at the early stages of lens placode formation, because the autoregulatory loop maintains Pax6 expression starting from this stage on (12,13). Thus, a reduction in Pax6 expression will be more prominent in cells in which only a single allele is active, resulting in a delay in the acquisition of critical threshold levels required for the onset of lens placode formation. Moreover, the development of the lens has been shown to be dependent on adjacent cell types (43), in which Pax6 is expressed as well. Specifically, here we demonstrate that Pax6 expression at its normal dosage is required for the size of the progenitor pool destined to an iris fate, which is adjacent to the germinative zone of the lens. Nevertheless, despite these abnormalities, we did not detect evidence for lens phenotype at E14.5 or in adult $Pax6^{flox/+}$*;α-Cre* mice (Fig. 3). We thus conclude that Pax6 dosage mediated by the α-enhancer is dispensable for lens development.

Reduction of Pax6 dosage in the lens only mildly affects iris development

Several lines of evidence indicate a major role for the lens in the development of the adjacent anterior chamber. Ablation of the lens, either mechanically (44,45) or by the expression of toxins (46,47), leads to aberrant formation of the anterior eye structures. Recent organ culture recombination experiments have shown that the chick lens can induce the expression of early markers of the peripheral mouse retina (34). The effect of Pax6 in the lens on the development of adjacent anterior ocular structures has been investigated by $Pax6^{+/-} \rightarrow Pax6^{+/+}$ chimera analysis. This approach revealed that up to 80% of the heterozygotic cells in the eye can be rescued by wild-type lens epithelium (20). These findings led to the notion that the abnormalities in the heterozygous eye are primarily due to autonomous deficiencies of Pax6 during early lens development (20).

Conditional mutagenesis allowed us to directly investigate the influence of Pax6 dosage reduction in the lens on the adjacent peripheral optic cup. Although severe lens and cornea abnormalities were observed in the $Pax6^{flox/+}$*;Le-Cre* mice, the iris morphology was comparable to normal based on the response to pilocarpine, the histology and the expression pattern of Sma (Fig. 6). Occasionally, however, irregular rim of the pupil was observed in adult $Pax6^{flox/+}$*;Le-Cre* mice (data not shown). This abnormality of the iris did not seem to occur during cell-fate determination in the iris primordium, as the size of the non-neuronal peripheral retina in the $Pax6^{flox/+}$*;Le-Cre* eyes was not reduced (Fig. 3). Thus, we conclude that the $Pax6^{+/-}$ lens is not affected with respect to its capacity for inducing anterior eye formation, and probably this mild iris phenotype is a result of the distorted lens size, which may lead to morphological disturbance of the adjacent iris simply because it cannot mechanically support the full iris length.

Pax6-distal^{high} as a size determinant of the iris progenitor pool

Establishment of the proximal–distal gradient of the optic cup seems to depend on the activity of the *Pax6* α-enhancer. This was suggested by the uniform distribution of β-gal in the optic cup of $Pax6^{lacZ}$ mutant mice, which are devoid of the *Pax6* α-enhancer (18). Here, we demonstrate that the enhanced Pax6 expression mediated by the α-enhancer is probably essential for establishing the size of the progenitor pool destined to iris fate. As early as E14.5, we observed a significant reduction (75% of control, Fig. 3) in the size of the non-neuronal peripheral retina. This size reduction was maintained in the iris length of the adult $Pax6^{flox/+}$*;α-Cre* mice (79% of control, Fig. 4).

There are several possible explanations for the retinal tips reduction. Potentially, the high concentration of Pax6 in the distal tips could inhibits neuronal cell differentiation, thus maintaining a pool of undifferentiated cells whose fate is determined later. This possibility is suggested by the observed correlation between Pax6^{high} and the lack of neuronal marker expression in the retinal tips (Fig. 3). However, the analysis of Pax6 distribution showed that in wild-type, the intensity of Pax6 expression at the border between the neuronal and non-neuronal compartments was on average 0.59 of the intensity at the most distal tips (d3 normal/d1 normal, Fig. 3). If the decision about the fate of the progenitors to neuronal or anterior ocular cell types was solely dependent on Pax6 concentration, neuronal cells would have been detected in the most distal retina of $Pax6^{flox/+}$*;α-Cre* eyes, in which the Pax6 dosage ranged from 0.53 to 0.63 of its dosage in the distal retina of normal mice (d2, d1 mutant/d1 normal, Fig. 3). However, the distal tips in $Pax6^{flox/+}$*;α-Cre* consist of non-neuronal cells and as in the normal optic cup, the neurons appear only toward the center of the retina (Fig. 3). Therefore, the decrease in the iris progenitor pool cannot be attributed to Pax6 levels alone and most probably involves other factors. Possible candidate mediators of the inhibition of neuronal cell differentiation are the bone morphogenic

protein (BMP)-4 and its putative target Msx1, which may inhibit neuronal cell differentiation while promoting an epidermal fate (48,49). These factors are expressed in the developing iris and inhibition of BMP-4 activity by noggin protein results in the absence of a CB and in the differentiation of ganglion cells instead (50). Because of the early death of the *Msx1* mutant mice, the role of Msx1 in anterior chamber development and its possible interaction with Pax6 has yet to be elucidated (51).

Another explanation for the observed reduction in the size of the $Pax6^{flox/+}$;*α-Cre* iris progenitors is that the reduction in Pax6 dosage may lead to a change in cell proliferation in $Pax6^{+/-}$ retinal progenitor cells, with a resulting reduction in the size of the progenitor pool of the whole distal retina (including both neuroretina and anterior ocular structure progenitors). Progenitor cells of both diencephalon and retina devoid of Pax6 show reduced proliferation (28,52). In contrast, E12 $Pax6^{sey/sey}$ cortical progenitors show accelerated proliferation and premature differentiation (53). Our comparison of the numbers of GFP^+ α-Cre-expressing cells per embryo in the $Pax6^{flox/+}$;*α-Cre* E14 eyes and in the eyes of control $Pax6^{+/+}$;*α-Cre* embryos showed only a mild, non-significant difference between the two genotypes. This implies that a reduction in Pax6 dosage does not lead to a general reduction in progenitor cell number but has a rather restricted effect on the iris progenitors.

Finally, yet another likely explanation for the observed reduction in size of the progenitor pool in $Pax6^{flox/+}$;*α-Cre* eyes is that at the most distal tips of the optic cup, a critical threshold level of Pax6 is required for cell-fate determination of the iris. A reduction in Pax6 dosage might result in delayed specification of the iris primordium, delayed iris development and eventually result in the iris hypoplasia.

Pax6–distal^{high} is required for the normal length of the adult iris

Analysis of the $Pax6^{flox/+}$;*α-Cre* mice revealed a significant reduction in the length of the iris in adults (to 79% of control). The reduction was evident at P4 (62% of control) and at E17 (83% of control). The more prominent reduction in iris size at P4 than in the adult mice may reflect the delay in muscle-cell differentiation occurring at this stage. Later in development, this delay is compensated for, as the iris appears to eventually acquire the normal proportion of muscle cells. The Pax, Dach, Eya and Six genetic network is reportedly employed in the context of somite myogenesis (54). Family members of these factors, Eya 1 (55), Six5 (56), Dach1 (57,58), are expressed in the embryonic mouse peripheral optic cup and recently, Pax3 expression has been detected in the developing iris in chick embryos (59). Thus, it is possible that in the distal retina, these factors, together with Pax6, function in the process of iris myogenesis and in the heterozygous mutants this process is delayed.

Pax6 is detected in the smooth muscle cells of the iris sphincter in mice (this study) and during muscle-cell differentiation in chick (59). We show here that Sma expression in $Pax6^{KO/+}$ and in the $Pax6^{flox/+}$;*α-Cre* mice is maintained despite the reduction in Pax6, and that the iris stroma is extensively reduced in this mice. Iris stroma cells do not seem to express Pax6, thus it is reasonable to speculate that the iris stroma defect is non-cell-autonomous event. Possibly, Pax6 in the developing iris regulates the expression of molecules required for the guidance or adhesion of the ocular mesenchyme to the iris stroma. Pax6 has indeed been implicated in the regulation of cephalic crest cells migration based on analysis of the homozygous rat Small-eye mutants (60,61) and in the regulation of cell-adhesion molecules, including N-cadherin in the lens (19) and R-cadherin in the brain (62). In future studies, the Cre/*loxP* approach will be instrumental for exploring the role of Pax6 dosage for the development of the iris stroma and the function of Pax6 in the mature smooth muscles of the iris, in which this evolutionary ancient transcription factor was recruited to function in a relatively new organ, which is unique to vertebrate species.

MATERIALS AND METHODS

Mouse lines

$Pax6^{flox/flox}$, *Le-Cre, α-Cre,* $Pax6^{KO/+}$ and the *Z/AP* reporter mice were established as described (13,23,26,28). $Pax6^{flox/+}$;*α-Cre* and littermate controls ($Pax6^{flox/+}$ or $Pax6^{+/+}$;*α-Cre*) were obtained by crossing $Pax6^{flox/+}$ with *α-Cre* mice. $Pax6^{flox/+}$;*Le-Cre* and littermate controls ($Pax6^{flox/+}$ or $Pax6^{+/+}$;*Le-Cre*) were obtained by crossing $Pax6^{flox/+}$ with *Le-Cre* mice. The day on which the copulatory plug was observed was defined as E0.5, and the day of birth was referred to as P1. Analyses were conducted on F1 progeny from a mating between ICR and FVB/NJ genetic backgrounds.

Histology and immunohistochemistry

Tissues were fixed in 4% paraformaldehyde at 4°C, dehydrated in a graded ethanol series and embedded in paraffin. Alternatively, fixed tissues were cryoprotected in a graded sucrose series and embedded in TBS buffer (Triangle Biomedical Sciences) or processed for embedding in Epon as described (7) Paraffin (10 μm) or semi-thin Epon sections (1 μm) were stained with hematoxylin and eosin (H&E) or Toluidine blue, respectively, using standard procedures (9). Frozen sections (14 μm) were stained with alkaline phosphatase as described (26). Frozen or dewaxed paraffin sections were examined immunohistochemically as described (13). The primary antibodies used were αPax6 (1:1000, Chemicon), α Sma (1:250, Sigma), αBrn3b (1:100, Santa Cruz) and αB-III tubulin (1:500, Chemicon). For staining of αPax6, αB-III tubulin and αBrn3b, sections were boiled twice in unmasking solution (Vector) prior to blocking. Secondary antibodies were conjugated to rhodamine red-X or to Cy2 (Jackson ImmunoResearch Laboratories). Slides were viewed with an Olympus BX61 fluorescent microscope and images were analyzed using the image analysis system 'AnalySIS'.

Measurements of lens diameter and iris size and morphology

Summary of the presented measurements is available in Supplementary Material, Table S1. To obtain position-matched

sections of the E14.5–E17.5 eyes, whole heads were embedded at a known orientation and transverse serial sections of the eyes were collected every 30 μm in regions where lens was detected. For postnatal stages, the positioning of enucleated eyes was carefully monitored, the eyes were positioned in parallel to the optic nerve and serial sections of 60 μm (adult) or 40 μm (P4) apart were collected. Measurements were conducted on sections with well-preserved morphology that included the pupil. The values for the presented indexes were averages from all sections of each eye. To overcome variance between different litters, we normalized all measured values by dividing them by the average value of the control littermates (*Pax6*$^{flox/+}$, *Pax6*$^{+/+}$, *Pax6*$^{+/+}$*;α-Cre* as indicated) in each litter.

Iris lengths in adult and P4 mice were measured from the CB to the sphincter. The proportion of iris muscle was calculated by measuring the Sma-positive area. For measurements of adult lens sizes, the isolated lenses were photographed using an MZFLIII fluorescent stereomicroscope (Leica). Images were analyzed using 'AnalySIS'. For examination of pupils, mice were deeply anesthetized by intraperitoneal injection of 2.5% avertine, and 4% pilocarpine eyedrops were instilled 4 min before they were killed. Alternatively, enucleated eyes were soaked in 4% pilocarpine for 6 min and then photographed.

Analysis of Pax6 distribution in the lens and optic cup

Pax6 staining intensity was measured from E14.5 serial eye sections 30 μm apart that contained the optic nerve head. Using a laser-scanning confocal microscope CLSM 410 (Zeiss), the averaged pixel intensity (values between 0 and 255) of Pax6 staining was measured at the lens epithelium of *Pax6*$^{flox/+}$*;Le-Cre* embryos and control littermates. The fluorescent intensities were calculated from signals above background using a threshold function. Sections in which the lens stalk was apparent were excluded from the calculations. The values were normalized by dividing them by Pax6 pixel averaged intensity in the retinal tips, which are not mutated in *Pax6*$^{flox/+}$*;Le-Cre* mutants. Normalized values were averaged for each eye. In *Pax6*$^{flox/+}$*;α-Cre* mice, we measured Pax6 intensity as described earlier in four discrete points of the distal retina and normalized them by division by the averaged pixel intensity of Pax6 in the cornea, which is not mutated in *Pax6*$^{flox/+}$*;α-Cre* mutants.

Counting of Cre-expressing GFP$^+$ retinal cells by FACS

Eyes were removed from embryos at E14.0 and dissected in Hanks' balanced salt solution. The eyes were digested with 25 units/ml papain (Sigma) followed by mild trituration. Dissociated cells were centrifuged at 200*g* for 2 min and resuspended in complete medium. GFP$^+$ cells were counted by FACS sorting (Becton Dickinson).

SUPPLEMENTARY MATERIAL

Supplementary Material is available at HMG Online.

ACKNOWLEDGEMENTS

The authors thank Dr Peter Gruss at the Max-Planck-Institute of Biophysical Chemistry in whose laboratory the *Pax6*^{flox}*, Le-Cre, α-Cre* and *Pax6*^{KO} were established, Dr Luc St-Onge for the *Pax6*^{KO} mice and Dr Corrine Lobe and Dr Andras Nagy for the *Z/AP* reporter line. The authors are grateful for suggestions on the manuscript by Dr Yosef Gruenbaum from the Hebrew University. R.A.-P.'s research is supported by the Israeli Academy of Sciences (401/02), Israeli Ministry of Health, Adams center for brain studies and is an Alon fellow. R.A.-P. and E.T. are supported by the German Israeli Foundation for Scientific Research and Development.

Conflict of Interest statement. None declared.

REFERENCES

1. Jimenez-Sanchez, G., Childs, B. and Valle, D. (2001) Human disease genes. *Nature*, **409**, 853–855.
2. Simpson, T.I. and Price, D.J. (2002) Pax6; a pleiotropic player in development. *Bioessays*, **24**, 1041–1051.
3. van Heyningen, V. and Williamson, K.A. (2002) PAX6 in sensory development. *Hum. Mol. Genet.*, **11**, 1161–1167.
4. Sisodiya, S.M., Free, S.L., Williamson, K.A., Mitchell, T.N., Willis, C., Stevens, J.M., Kendall, B.E., Shorvon, S.D., Hanson, I.M., Moore, A.T. *et al.* (2001) PAX6 haploinsufficiency causes cerebral malformation and olfactory dysfunction in humans. *Nat. Genet.*, **28**, 214–216.
5. Yasuda, T., Kajimoto, Y., Fujitani, Y., Watada, H., Yamamoto, S., Watarai, T., Umayahara, Y., Matsuhisa, M., Gorogawa, S., Kuwayama, Y. *et al.* (2002) PAX6 mutation as a genetic factor common to aniridia and glucose intolerance. *Diabetes*, **51**, 224–230.
6. Glaser, T.D., Walton, S., Cai, J., Epstein, J., Jepeal, L. and Mass, R.L. (1995) *Pax6* gene mutations in aniridia. In *Molecular Genetics of Ocular Diseases.* Wiley Liss, New York, pp. 51–82.
7. Baulmann, D.C., Ohlmann, A., Flugel-Koch, C., Goswami, S., Cvekl, A. and Tamm, E.R. (2002) Pax6 heterozygous eyes show defects in chamber angle differentiation that are associated with a wide spectrum of other anterior eye segment abnormalities. *Mech. Dev.*, **118**, 3–17.
8. Pei, Y.F. and Rhodin, J.A. (1970) The prenatal development of the mouse eye. *Anat. Rec.*, **168**, 105–125.
9. Smith, R.S. (2002) *Systematic evaluation of the mouse eye.* CRC Press.
10. McAvoy, J.W., Chamberlain, C.G., de Iongh, R.U., Hales, A.M. and Lovicu, F.J. (1999) Lens development. *Eye*, **13** (Pt 3b), 425–437.
11. Walther, C. and Gruss, P. (1991) *Pax-6*, a murine paired box gene, is expressed in the developing CNS. *Development*, **113**, 1435–1449.
12. Grindley, J.C., Davidson, D.R. and Hill, R.E. (1995) The role of Pax-6 in eye and nasal development. *Development*, **121**, 1433–1442.
13. Ashery-Padan, R., Marquardt, T., Zhou, X. and Gruss, P. (2000) Pax6 activity in the lens primordium is required for lens formation and for correct placement of a single retina in the eye. *Genes Dev.*, **14**, 2701–2711.
14. Macdonald, R. and Wilson, S.W. (1997) Distribution of Pax6 protein during eye development suggests discrete roles in proliferative and differentiated visual cells. *Dev. Genes Evol.*, **206**, 363–369.
15. Nishina, S., Kohsaka, S., Yamaguchi, Y., Handa, H., Kawakami, A., Fujisawa, H. and Azuma, N. (1999) PAX6 expression in the developing human eye. *Br. J. Ophthalmol.*, **83**, 723–727.
16. Lewis, W. (1903) Wandering pigment cells arising from the epithelium of the optic cup, with observations on the origin of the muscle sphincter pupillae in the chick. *J. Am. Anat.*, **2**, 405–416.
17. Cvekl, A. and Tamm, E.R. (2004) Anterior eye development and ocular mesenchyme: new insights from mouse models and human diseases. *Bioessays*, **26**, 374–386.
18. Baumer, N., Marquardt, T., Stoykova, A., Ashery-Padan, R., Chowdhury, K. and Gruss, P. (2002) Pax6 is required for establishing naso-temporal and dorsal characteristics of the optic vesicle. *Development*, **129**, 4535–4545.

19. van Raamsdonk, C.D. and Tilghman, S.M. (2000) Dosage requirement and allelic expression of PAX6 during lens placode formation. *Development*, **127**, 5439–5448.
20. Collinson, J.M., Quinn, J.C., Buchanan, M.A., Kaufman, M.H., Wedden, S.E., West, J.D. and Hill, R.E. (2001) Primary defects in the lens underlie complex anterior segment abnormalities of the Pax6 heterozygous eye. *Proc. Natl Acad. Sci. USA*, **98**, 9688–9693.
21. Genis-Galvez, J.M. (1966) Role of the lens in the morphogenesis of the iris and cornea. *Nature*, **210**, 209–210.
22. Beebe, D.C. (1986) Development of the ciliary body: a brief review. *Trans. Ophthalmol. Soc. UK*, **105** (Pt 2), 123–130.
23. St-Onge, L., Sosa-Pineda, B., Chowdhury, K., Mansouri, A. and Gruss, P. (1997) Pax6 is required for differentiation of glucagon-producing alpha-cells in mouse pancreas. *Nature*, **387**, 406–409.
24. Kammandel, B., Chowdhury, K., Stoykova, A., Aparicio, S., Brenner, S. and Gruss, P. (1999) Distinct *cis*-essential modules direct the time-space pattern of the Pax6 gene activity. *Dev. Biol.*, **205**, 79–97.
25. Ashery-Padan, R., Zhou, X., Marquardt, T., Herrera, P., Toube, L., Berry, A. and Gruss, P. (2004) Conditional inactivation of Pax6 in the pancreas causes early onset of diabetes. *Dev. Biol.*, **269**, 479–488.
26. Lobe, C.G., Koop, K.E., Kreppner, W., Lomeli, H., Gertsenstein, M. and Nagy, A. (1999) Z/AP, a double reporter for cre-mediated recombination. *Dev. Biol.*, **208**, 281–292.
27. Ashery-Padan, R. (2002) Somatic gene targeting in the developing and adult mouse retina. *Methods*, **28**, 457–464.
28. Marquardt, T., Ashery-Padan, R., Andrejewski, N., Scardigli, R., Guillemot, F. and Gruss, P. (2001) Pax6 is required for the multipotent state of retinal progenitor cells. *Cell*, **105**, 43–55.
29. Dimanlig, P.V., Faber, S.C., Auerbach, W., Makarenkova, H.P. and Lang, R.A. (2001) The upstream ectoderm enhancer in Pax6 has an important role in lens induction. *Development*, **128**, 4415–4424.
30. Hanson, I.M., Fletcher, J.M., Jordan, T., Brown, A., Taylor, D., Adams, R.J., Punnett, H.H. and van Heyningen, V. (1994) Mutations at the PAX6 locus are found in heterogeneous anterior segment malformations including Peters' anomaly. *Nat. Genet.*, **6**, 168–173.
31. Stone, D.L., Kenyon, K.R., Green, W.R. and Ryan, S.J. (1976) Congenital central corneal leukoma (Peters' anomaly). *Am. J. Ophthalmol.*, **81**, 173–193.
32. van Raamsdonk, C.D. and Tilghman, S.M. (2001) Optimizing the detection of nascent transcripts by RNA fluorescence in situ hybridization. *Nucleic Acids Res.*, **29**, E42–2.
33. Lee, M.K., Tuttle, J.B., Rebhun, L.I., Cleveland, D.W. and Frankfurter, A. (1990) The expression and posttranslational modification of a neuron-specific beta-tubulin isotype during chick embryogenesis. *Cell Motil. Cytoskeleton*, **17**, 118–132.
34. Thut, C.J., Rountree, R.B., Hwa, M. and Kingsley, D.M. (2001) A large-scale *in situ* screen provides molecular evidence for the induction of eye anterior segment structures by the developing lens. *Dev. Biol.*, **231**, 63–76.
35. Gould, D.B. and John, S.W. (2002) Anterior segment dysgenesis and the developmental glaucomas are complex traits. *Hum. Mol. Genet.*, **11**, 1185–1193.
36. Gould, D.B., Smith, R.S. and John, S.W. (2004) Anterior segment development relevant to glaucoma. *Int. J. Dev. Biol.*, **48**, 1015–1029.
37. Plaza, S., Dozier, C., Langlois, M.C. and Saule, S. (1995) Identification and characterization of a neuroretina-specific enhancer element in the quail *Pax-6* (Pax-QNR) gene. *Mol. Cell. Biol.*, **15**, 892–903.
38. Williams, S.C., Altmann, C.R., Chow, R.L., Hemmati-Brivanlou, A. and Lang, R.A. (1998) A highly conserved lens transcriptional control element from the *Pax-6* gene. *Mech. Dev.*, **73**, 225–229.
39. Xu, Z.P. and Saunders, G.F. (1998) PAX6 intronic sequence targets expression to the spinal cord. *Dev. Genet.*, **23**, 259–263.
40. Xu, P.X., Zhang, X., Heaney, S., Yoon, A., Michelson, A.M. and Maas, R.L. (1999) Regulation of Pax6 expression is conserved between mice and flies. *Development*, **126**, 383–395.
41. Kleinjan, D.A., Seawright, A., Schedl, A., Quinlan, R.A., Danes, S. and van Heyningen, V. (2001) Aniridia-associated translocations, DNase hypersensitivity, sequence comparison and transgenic analysis redefine the functional domain of PAX6. *Hum. Mol. Genet.*, **10**, 2049–2059.
42. Griffin, C., Kleinjan, D.A., Doe, B. and van Heyningen, V. (2002) New 3′ elements control Pax6 expression in the developing pretectum, neural retina and olfactory region. *Mech. Dev.*, **112**, 89–100.
43. Coulombre, J.L. and Coulombre, A.J. (1963) Lens development: fiber elongation and lens orientation. *Science*, **142**, 1489–1490.
44. Coulombre, A.J. and Coulombre, J.L. (1964) Lens development, I. Role of the lens in eye growth. *J. Exp. Zool.*, **156**, 39–47.
45. Beebe, D.C. and Coats, J.M. (2000) The lens organizes the anterior segment: specification of neural crest cell differentiation in the avian eye. *Dev. Biol.*, **220**, 424–431.
46. Breitman, M.L., Bryce, D.M., Giddens, E., Clapoff, S., Goring, D., Tsui, L.C., Klintworth, G.K. and Bernstein, A. (1989) Analysis of lens cell fate and eye morphogenesis in transgenic mice ablated for cells of the lens lineage. *Development*, **106**, 457–463.
47. Harrington, L., Klintworth, G.K., Secor, T.E. and Breitman, M.L. (1991) Developmental analysis of ocular morphogenesis in alpha A-crystallin/diphtheria toxin transgenic mice undergoing ablation of the lens. *Dev. Biol.*, **148**, 508–516.
48. Wilson, P.A. and Hemmati-Brivanlou, A. (1995) Induction of epidermis and inhibition of neural fate by Bmp-4. *Nature*, **376**, 331–333.
49. Suzuki, A., Ueno, N. and Hemmati-Brivanlou, A. (1997) *Xenopus msx1* mediates epidermal induction and neural inhibition by BMP4. *Development*, **124**, 3037–3044.
50. Zhao, S., Chen, Q., Hung, F.C. and Overbeek, P.A. (2002) BMP signaling is required for development of the ciliary body. *Development*, **129**, 4435–4442.
51. Satokata, I. and Maas, R. (1994) Msx1 deficient mice exhibit cleft palate and abnormalities of craniofacial and tooth development. *Nat. Genet.*, **6**, 348–356.
52. Warren, N. and Price, D.J. (1997) Roles of Pax-6 in murine diencephalic development. *Development*, **124**, 1573–1582.
53. Estivill-Torrus, G., Pearson, H., van Heyningen, V., Price, D.J. and Rashbass, P. (2002) Pax6 is required to regulate the cell cycle and the rate of progression from symmetrical to asymmetrical division in mammalian cortical progenitors. *Development*, **129**, 455–466.
54. Heanue, T.A., Reshef, R., Davis, R.J., Mardon, G., Oliver, G., Tomarev, S., Lassar, A.B. and Tabin, C.J. (1999) Synergistic regulation of vertebrate muscle development by Dach2, Eya2, and Six1, homologs of genes required for *Drosophila* eye formation. *Genes Dev.*, **13**, 3231–3243.
55. Xu, P.X., Woo, I., Her, H., Beier, D.R. and Maas, R.L. (1997) Mouse Eya homologues of the *Drosophila* eyes absent gene require Pax6 for expression in lens and nasal placode. *Development*, **124**, 219–231.
56. Klesert, T.R., Cho, D.H., Clark, J.I., Maylie, J., Adelman, J., Snider, L., Yuen, E.C., Soriano, P. and Tapscott, S.J. (2000) Mice deficient in Six5 develop cataracts: implications for myotonic dystrophy. *Nat. Genet.*, **25**, 105–109.
57. Caubit, X., Thangarajah, R., Theil, T., Wirth, J., Nothwang, H.G., Ruther, U. and Krauss, S. (1999) Mouse Dac, a novel nuclear factor with homology to *Drosophila* dachshund shows a dynamic expression in the neural crest, the eye, the neocortex, and the limb bud. *Dev. Dyn.*, **214**, 66–80.
58. Heanue, T.A., Davis, R.J., Rowitch, D.H., Kispert, A., McMahon, A.P., Mardon, G. and Tabin, C.J. (2002) Dach1, a vertebrate homologue of *Drosophila* dachshund, is expressed in the developing eye and ear of both chick and mouse and is regulated independently of Pax and Eya genes. *Mech. Dev.*, **111**, 75–87.
59. Jensen, A.M. (2005) Potential roles for *BMP* and *Pax* genes in the development of iris smooth muscle. *Dev. Dyn.*, **232**, 385–392.
60. Matsuo, T., Osumi-Yamashita, N., Noji, S., Ohuchi, H., Koyama, E., Myokai, F., Matsuo, N., Taniguchi, S., Doi, H., Iseki, S. *et al.* (1993) A mutation in the *Pax-6* gene in rat small eye is associated with impaired migration of midbrain crest cells. *Nat. Genet.*, **3**, 299–304.
61. Osumi-Yamashita, N., Kuratani, S., Ninomiya, Y., Aoki, K., Iseki, S., Chareonvit, S., Doi, H., Fujiwara, M., Watanabe, T. and Eto, K. (1997) Cranial anomaly of homozygous rSey rat is associated with a defect in the migration pathway of midbrain crest cells. *Dev. Growth Differ.*, **39**, 53–67.
62. Stoykova, A., Gotz, M., Gruss, P. and Price, J. (1997) Pax6-dependent regulation of adhesive patterning, R-cadherin expression and boundary formation in developing forebrain. *Development*, **124**, 3765–3777.